Pathology & Oncology Research (2020) 26:2177–2183
https://doi.org/10.1007/s12253-020-00805-3

ORIGINAL ARTICLE

Comparison of Different Colorectal Cancer With Liver Metastases Models Using Six Colorectal Cancer Cell Lines

Yuting Xu[1] · Lin Zhang[1] · Qingling Wang[1] · Maojin Zheng[1]

Received: 19 May 2019 / Accepted: 4 March 2020 / Published online: 14 March 2020
© Arányi Lajos Foundation 2020

Abstract

At present, modeling methods of colorectal cancer with liver metastases have significant limitations. Here, we established orthotopic and ectopic hepatic metastases models using six colorectal cancer cell lines to choose an ideal animal model for studying colorectal cancer growth and liver metastases. Luciferin-expressing six colorectal cancer cell lines were used to induce animal models of colorectal cancer with liver metastases by intra-splenic injection or implantation of tumor tissue in the caecum. Tumors growth and metastatic events were observed by bioluminescence imaging. In orthotopic transplantation group, six cell lines all had taken rates of 100% for orthotopic tumors but showed variations in rates of growth. HCT-116 cell developed the 50% liver metastases. However, the ectopic transplantation group achieved higher liver metastatic rate, with the highest frequencies for HCT116 cell (90%) and SW620 cell (77.8%). Furthermore, the time to develop liver metastases and survival rates of bearing-tumor mice were shorter than orthotopic transplantation group. Additionally, six colorectal cancer cell lines resulted in more lymph node metastases in orthotopic transplantation group, whereas produced widespread peritoneal seeding in ectopic transplantation group. Bioluminescence imaging and pathological findings confirmed the growth and metastatic characteristics of tumors. Two animal models of colorectal cancer using six cell lines showed highly variations in rates of growth, survival rates of bearing-tumor mice and frequencies of metastases. The study provides useful information for the establishment of clinically relevant colorectal cancer with liver metastases animal models.

Keywords Colorectal cancer cell lines · Liver metastases · Orthotopic model · Ectopic model

Introduction

Colorectal cancer (CRC) is the third most commonly diagnosed cancer in males and the second in females, it is estimated that there will be 1.4 million cases and 693,900 deaths attributable to this disease in 2012 [1, 2]. Despite presenting with a resectable primary tumor, 20–25% patients progress to distant metastases, mainly to liver, 5-year survival rate of patients diagnosed with distant metastases decreases to less than 10% [3, 4]. Therefore, there is an urgent need for new treatment strategies to improve the prognosis of CRC patients with liver metastases. Animals models are essential to the mechanistic research and development of effective therapeutics. At present, metastatic disease can be modeled using orthotopic implantation and ectopic implantation. The former includes injection of CRC cells or implantation of tumor tissue in the colon, cecum or the rectal wall [5–9], and the latter is composed of subcutaneous, intra-splenic injection (splenectomy performed after tumor cell injection or not) [10], implantation of a small piece of tumor tissue into the liver parenchyma or subcapsule, injection of tumor cells by intra-portal [11, 12]. There are also chemically-induced mouse models [13] and genetically-engineered models [14]. Due to obvious variation in results between different laboratories, the difficulty for researchers in selecting animal models increased significantly.

Attribute to strong specificity, high sensitivity and less environmental pollution, bioluminescence imaging technology (BLI) in vivo has been widely used in all kinds of tumor's studies [15], including CRC [16, 17]. It can be used to characterize the characteristics of tumor growth, invasion and metastases by testing the intensity of the bioluminescence expression in animal models.

✉ Yuting Xu
xyt325@xzhmu.edu.cn

[1] Department of Pathology, Xuzhou Medical University, 221004 Xuzhou, Jiangsu, China

The aim of this study was to establish orthotopic and ectopic CRC with liver metastases models in nude mice with luciferase-expressing six human CRC cell lines, so as to compare the difference of between the two animal models and provide useful background information on the six CRC cell lines in clinically relevant orthotopic and ectopic tumor models.

Materials and Methods

Main Reagents LEIBOVITZ'S L-15, DMEM, RPMI 1640 and McCoy's 5A medium and fetal bovine serum (FBS) were from GIBCO company (Grand Island, USA). Streptomycin and penicillin were purchased from Life Technologies (Inc., Grand Island, NY). Puromycin was bought from Sigma-Aldrich (St. Louis, MO, USA). Firefly luciferase-lentiviruses and Polybrene were obtained from GENECHEM (Shanghai, China). D-luciferin potassium salt was obtained from PROMEGA (Madison, WI, USA). Medical anastomosis glue was obtained from Bai Yun Mountain Pharmaceutical Company (Guangzhou, China). HBSS was from GIBCO company (Grand Island, USA).

Cell Culture Six generally available human CRC cell lines, SW620, SW480, HCT116, HT29, LOVO and DLD1, were all obtained from the Shanghai Institute of Biochemistry and Cell Biology, Chinese Academy of Sciences (Shanghai, China). All cell lines expressed seven oncogenes, including c-*myc*, N-*ras*, H-*ras*, K-*ras*, *p53*, *myb* and *fos*. However, two oncogenes, *sis* and *SNRPA1*, displayed differential expression among these colorectal cell lines [18, 19]. Cell lines were maintained in LEIBOVITZ'S L-15, DMEM and RPMI 1640 and McCoy's 5A medium, respectively, supplemented with 10% FBS,100 μg/ml streptomycin and 100 unit/ml penicillin and were infected with lentiviruses carrying firefly luciferase with 8 μg/mL Polybrene in media. After a 48 h incubation, the transduced cells were selected with 2–6 μg/mL of Puromycin for 7–10 days.

Animals 4-6-week-old male or female athymic BALB/c nude mice were used and maintained under specific pathogen-free conditions at room temperature.

Xenograft Models For the implantation of tumor tissue in the caecum, 1×10^6 luciferase-expressing SW620, SW480, HCT116, HT29, LOVO and DLD1 tumor cells were injected into left flanks of 4 animals to establish subcutaneous xenografts. An incision was made on the middle of the lower abdomen and the cecum was picked-out after nude mice were anesthetized. Subsequently, a single tumor fragment, an average size of 1 mm^3, which was obtained from subcutaneous grown tumors, was conglutinated to serosa of the wall of cecum using medical anastomosis glue following scraping of the serosa surface. After implantation, the abdominal incision was closed in two-layer suture using 6–0 nylon surgical sutures. Each cell line was implanted in a series of 10 mice.

For the intra-splenic injection, nude mice were anesthetized with pentobarbital sodium (1.5 mg/20 g body weight) by an intraperitoneal injection. A small left abdominal flank incision was made to expose the spleen, 3×10^6 luciferase-tagged SW620, SW480, HCT116, HT29, LOVO and DLD1 cells in 50 μL HBSS were injected into the spleen slowly using a 32 G needle. Subsequently, a cotton swab was held over the injection site and gently massaged the spleen over 5 min to avoid extravasations and promote tumor cells back into the liver. And then the spleen was excised via ligation at the hilum of the spleen. Each cell line was injected in a series of 10 mice.

Bioluminescence Imaging Monitors Tumor Growth and Metastases All the cells were traced using an IVIS Lumina imaging system (Caliper, Hopkinton, MA, USA) at 2 days and 7 days after the injection, and then the mice were observed twice per week. Mice received intraperitoneal injection of D-luciferin potassium salt solution at a dose of 150 mg/kg according to manufacturer instructions. Subsequently, animals were anesthetized with 1% isoflurane and imaging acquisition was performed at 10 min after luciferin injection. Living Image software (Caliper) was used to quantify the luciferase activity. Tumor-bearing animals were killed based on tumor size (luminescence efficiency reached 1×10^{11} photons), the mice exhibited signs of systemic decline (obstruction, cachexia, or any other clinical decompensation) or 8 weeks after transplantation.

Hematoxylin and Eosin Staining Mice autopsy was conducted to examine primary and distant organ metastatic tumor nodules. Tumor samples were collected for histological examination. Tissues were fixed in 4% paraformaldehyde, embedded in Paraffin for Hematoxylin and Eosin (H&E) staining, which was performed according to the standard procedures.

Statistical Analysis The quantified bioluminescence intensity of the tumors were reported as mean ± standard deviation. Data analyses were performed using GraphPad Prism version 7.0 (Inc., La Jolla, ca., USA). Statistical differences were termed as $P < 0.05$.

Results

Tumorigenesis by Orthotopic Transplantation

Orthotopic tumors were detected in all animals after the tumors tissue were implanted in the cecum. Quantification of

bioluminescence intensity demonstrated rapid and consistent rise of tumor growth over time in our models, and tumors rate of growth were varied considerably between six cell lines (Fig. 1a-c). DLD1 cell exhibited the biggest tumors volume in the caecum and following the shortest survival periods in six cell lines, whereas HT29 cell presented the opposite result. Intermediate rate of growth and survival periods were observed for HCT116, SW620, SW480 and LOVO cell lines (Fig. 1a-c; Table 1). Liver metastases were detected at 22–34 days after implantation and in 0–50% of tumor-bearing mice, with the highest frequencies for HCT116 cell (5 of 10 mice) (Fig. 1d-e). The following are SW620 cell (3 of 10 mice) and LOVO cell (2 of 9 mice) (Fig. 1d-e). HT29 cell had no liver metastases but showed the highest lymph node metastases rates (50%) and peritoneal seeding (20%), whereas intermediate take rates of mesenteric lymph node metastases were observed for HCT116 cell (40%), LOVO cell (33.3%) and SW620 cell (30%). SW480 cell and DLD1 cell without liver metastases, lymph node metastases and peritoneal seeding in orthotopic transplantation group (Fig. 1d-e; Table 1). Lung metastases were not detected in any of cases (Table 1).

Tumorigenesis by Ectopic Transplantation

According to the preliminary experiment results, 3×10^6 cancer cell were injected for each mouse. Unexpectedly, 1–2 mice in the four cell lines-injected groups (SW620, SW480, HT29 and LOVO) died within 3 days after injection. The survival rates of tumor-bearing mice were shorter than orthotopic transplantation group and slightly different between the six tumor cells (Table 2). Two days after injection, we did not find the liver-colonization of tumor cells, 5 mice from SW620 cells and 4 mice from HCT116 cells developed

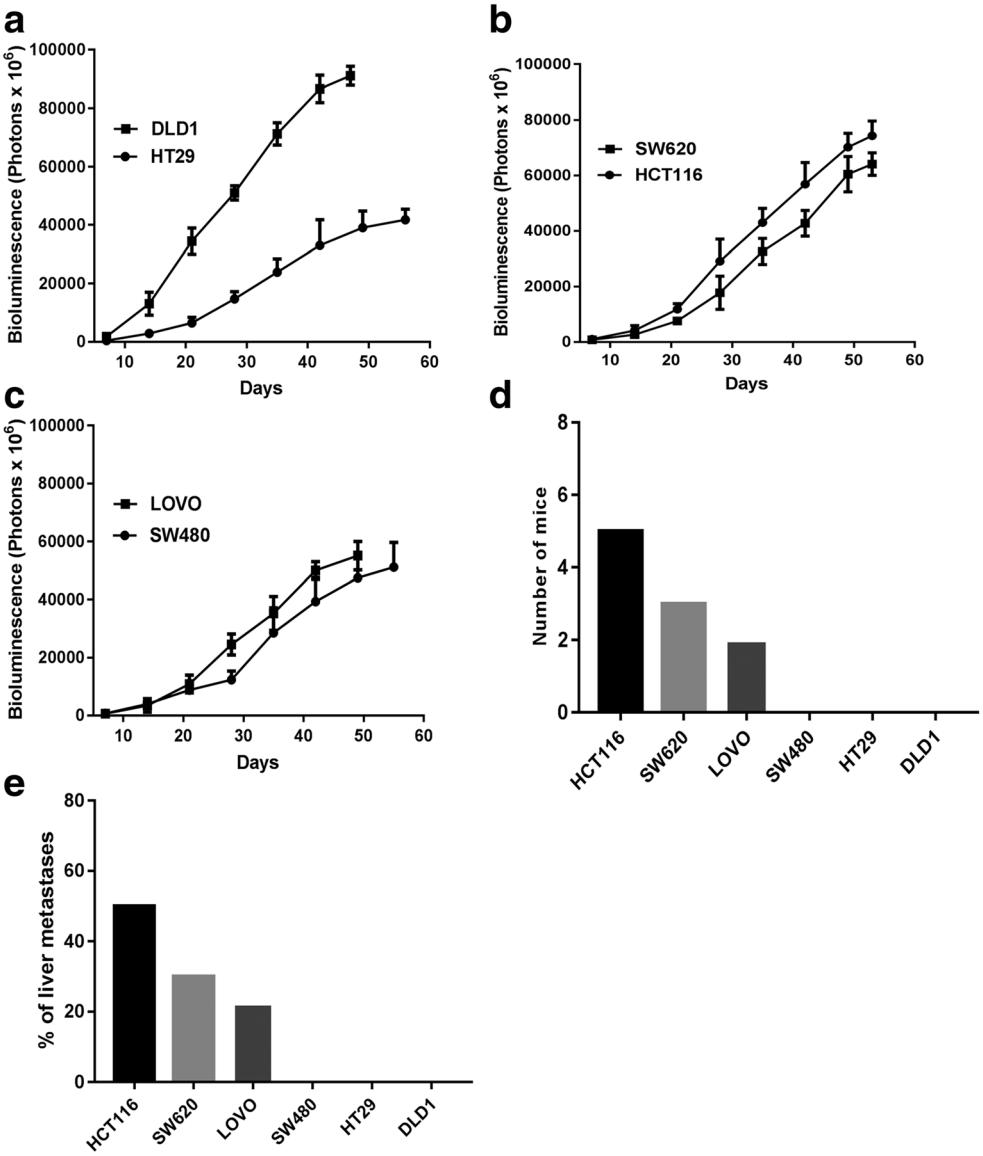

Fig. 1 Bioluminescence monitors tumor burden growth and liver metastases in the orthotopic transplantation group. **a** Nude mice underwent surgical implantation of tumor tissue from luciferase-expressing DLD1 and HT29 cell lines in the cecum wall. Photon counts allow quantification of tumors burden in the cecum wall (n= 10, mean ± SE). **b** The quantified bioluminescence signal demonstrated the growth of tumors from SW620 and HCT116 cell lines (n=10, mean ± SE). **c** The quantified bioluminescence signal demonstrated the growth of tumors from LOVO and SW480 cell lines (n= 9 in LOVO cell group, n= 10 in SW480 cell group, mean ± SE). **d** The number of animals proceed to develop into liver metastases via six CRC cell lines. **e** The percentage of animals within each cell model that developed liver metastatic disease (n=9 in LOVO cell group, n=10 in the others cell groups)

Table 1 Detailed results for orthotopic implantation of tumor tissue in the caecum

Cells	mice	Survival days	Take rate※	Dissemination site (Number of mice %)		
		Median value	Number of mice(%)	Lung	Lymphatic	Seeding
HCT116	10	51.3(8.7–12.1)	10/10 (100.0)	0/10 (0.0)	4/10 (40.0)	1/10(10.0)
HT29	10	55.9(6.0–11.9)	10/10 (100.0)	0/10 (0.0)	5/10 (50.0)	2/10(20.0)
SW620	10	52.2(4.5–14.0)	10/10 (100.0)	0/10 (0.0)	3/10 (30.0)	1/10(10.0)
SW480	10	53.6(8.7–12.1)	10/10 (100.0)	0/10 (0.0)	0/10 (0.0)	0/10(0.0)
LOVO	9*	50.7(6.7–10.3)	9/9 (100.0)	0/9 (0.0)	3/9 (33.3)	1/9(11.1)
DLD1	10	45.8 (3.2–9.2)	10/10 (100.0)	0/10(0.0)	0/10 (0.0)	0/10(0.0)

*One out of ten animals was dead within 7 days after implantation

※ Tumors in the caecum

hepatic sites at 7 days after injection. Other groups (SW480, HT29, LOVO and DLD1 cells) appeared liver metastases at 10–21 days after the injection. In total, the liver metastases were detected in 20–90% of tumor-bearing mice, with the highest frequencies for HCT116 cell (9 of 10 mice) and SW620 cell (7 of 9 mice) (Fig. 2a-b), and the rates of tumor growth were similar in two groups. Compared to HCT116 and SW620 tumor-bearing mice, other groups (SW480, HT29, LOVO and DLD1 cells) presented a lower rates of liver metastases (Fig. 2a-b).

Lymph node metastases were found in four cell groups (SW620, HCT116, HT29 and LOVO cells). Both SW620 cell and HT29 cell demonstrated 33.3% lymph node metastases (3 of 9 mice), the other two groups demonstrated 10–25% lymphatic metastasis (1 of 10 mice in the HCT116-group and 2 of 8 mice in the LOVO-group) (Table 2). Interestingly, all the groups had a peritoneal seeding, the highest frequencies were found in the LOVO group (3 of 8 mice), which only with 50% liver metastases (Table 2; Fig. 2b). Only one case of SW620 cell had lung metastases (Table 2).

Histological Assays

All tumor samples were examined by autopsy and microscopic examination to evaluate growth and metastatic characteristics. Orthotopic tumors presented exophytic masses with invasive growth at the wall of cecum.They were poorly demarcated from the surrounding tissue (Fig. 3a). Multiple small metastatic nodules (1–5 mm) were found in the parenchyma of the liver lobe, but single large nodule (10 mm) was also found. Metastatic tumors had no capsule, with necrosis in the center of nodules in a few cases (Fig. 3b). Compared to normal tissue, metastatic mesenteric lymph nodes with larger volume and harden texture. Peritoneal carcinomatosis showed multiple small nodules (1–7 mm) attached to the peritoneal surface.

Morphologic observation indicated that xenografts recreated the malignant tumor architecture and growth characteristics. Tumor tissue penetrated into the wall of the caecum, some to the extent in the lumen of the caecum, hepatic or lung parenchyma. Both the tumor cells and the nuclei showed pleomorphic variation (Fig. 3c-d). We also examined the intravasation potential of six CRC cell lines in orthotopic primary tumors. Regrettably, we only found microvascular invasion of HCT116 and SW620 cell lines (Fig. 3e).

Discussion

In this study, we developed two different CRC with liver metastases models using intra-splenic injection of cancer cells

Table 2 Detailed results for ectopic implantation experiments from intra-splenic injections

Cells	Mice	Survival days	Dissemination site (Number of mice %)		
		Median value	Lung	Lymphatic	Seeding
HCT116	10	41.3 (3.3–8.4)	0/10 (0.0)	1/10 (10.0)	3/10(30.0)
HT29	9*	48.5 (2.7–7.1)	0/9 (0.0)	3/9(33.3)	3/9(33.3)
SW620	9*	38.2 (6.4–11.2)	1/9 (11.1)	3/9(33.3)	2/9(22.2)
SW480	8*	51.7 (9.1–14.3)	0/8 (0.0)	0/8 (0.0)	1/8(12.5)
LOVO	8*	46.5 (4.6–15.4)	0/8 (0.0)	2/8(25.0)	3/8(37.5)
DLD1	10	53.4 (3.7–10.7)	0/10 (0.0)	0/10 (0.0)	2/10(20.0)

*One or two out of ten animals were dead within 3 days after injection

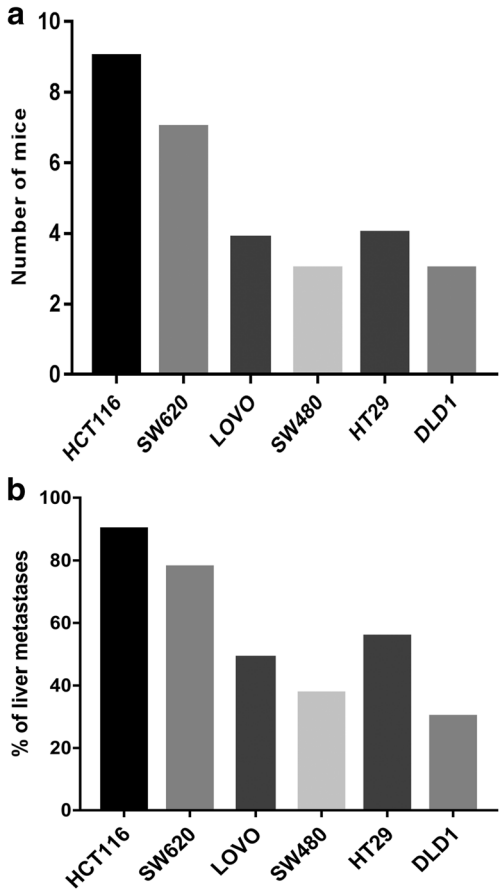

Fig. 2 Liver metastases in the ectopic transplantation group. **a** The number of animals proceed to develop into liver metastases via six CRC cell lines. **b** The percentage of animals within each cell model that developed liver metastatic disease (n=10 in HCT116 and DLD1 cell groups, n=9 in HT29 and SW620 cell groups, n=8 in SW480 and LOVO cell groups)

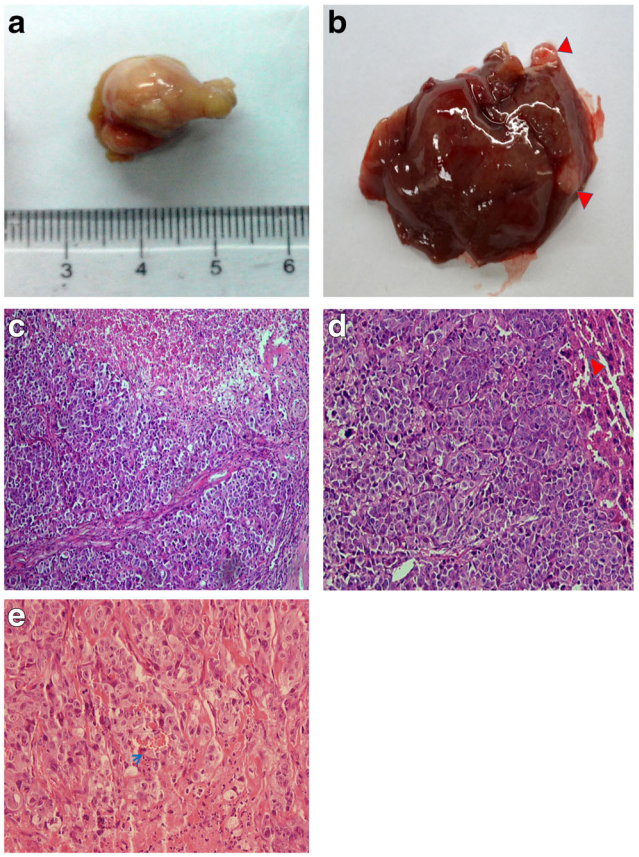

Fig. 3 Primary tumors and liver metastatic tumors in orthotopic and ectopic model groups. **a** Representative necropsy photograph of primary tumors in the cecum wall from luciferase-tagged HCT116 cell was shown. **b** Representative photograph of liver metastases from HCT116 cell. Arrows indicated tumor formation in the liver. **c** H&E section of primary tumor from SW620 cell showed tumor pleomorphic variation and necrosis (magnification 100). **d** H&E section of the mouse liver depicts tumor metastases from SW620 cell. Arrows indicated the normal liver tissue (magnification 200). **e** H&E section of the intravasation of HCT116 cell in orthotopic primary tumors. Arrows indicated the intravasation of tumor cells (magnification 400)

and implantation of tumor tissue in the caecum, which are two common techniques to establish mouse CRC metastatic tumors. Six human CRC cell lines showed large variations in rate of tumors' growth, survival periods of tumor-bearing mouse, the time of metastatic tumor formation and frequency of metastases.

Firstly, we established an orthotopic animal models by implantation of tumor tissue in the serosa of caecum. Although it appears likely that tumor cells via caecum injection in the mucosal surface will more mimic the route of CRC growth and dissemination in humans, it is technically difficult and carriers a tumor cell leakage risk or spillage within the lumen [20–22]. Meanwhile, some studies had demonstrated that CRC orthotopic xenografts on the intestinal serosa appears to lead to more reproducible liver metastases [23, 24]. In six CRC cell lines, HCT116 cell, with intermediate rate of growth, however, had developed the highest frequencies of hepatic metastases (50%). It might be attributed to the six cell lines are characterized by various driver oncogens [18, 19] or tumor burden caused disease symptoms before metastases. Meanwhile, previous reports had demonstrated that the intravasation plays an important role in the early stages of tumor metastasis [25]. Therefore, we examined the intravasation potential of six CRC cell lines in orthotopic primary tumors by the microscopy. Regrettably, we only found intravasation of and HCT116 and SW620 cell lines. Combined to our liver metastasis results, we have reason to believe that intravasation promotes liver metastasis of HCT116 cell and SW620 cell lines. Although no definite intravasation was found in other CRC cell lines, the effect of observation time and the quantity of tissue specimen could not be ruled out. K. Flatmark. and colleagues [26] studied twelve human colon cancer cell lines, including HT29, SW480 and SW620 cell lines, in a similar orthotopic model, and found the similar low rates of liver metastases (0–20%). However, for HCT116 cell, liver metastatic finding in tumor-bearing mice was not observed, which had a great discrepancy with our

results. In some studies with orthotopic xenografts, rates of liver metastases from HCT116 cell were in the range from 47% to 71% [8, 27]. These results are similar to our study. This phenomenon implies the observed difference in vivo with the same cell line in common experience between different laboratories. The most likely explanation for this discrepancy is that different characteristics of cell line in different laboratories. Additionally, it could be ascribed to use of different strains of mice and we also cannot be ruled out the influence of the intestine or liver microenvironment on CRC cell lines [28–30].

Secondly, intra-splenic injection showed rapid liver metastatic tumor formation and the higher hepatic metastatic rate than orthotopic transplantation group. One possible reason is that the technology directly mimics the generally process of CRC hematogenous metastasis, which is easier to form liver colonization. This hypothesis has been confirmed in our study. We found that liver colonization of most CRC cells occurred in earlier period in intra-splenic injection group than orthotopic animal models group, the outstanding representatives were HCT116 cell and SW620 cell. Lee et al. [10] study also showed that HCT116 appeared 100% hepatic dissemination after 14 days from intra-splenic injections, which has no obvious differences with our research results. The reason for HCT116 cells consistently produced hepatic metastasis maybe attributed to the more efficient adhesion potential to fibronectin (FN) and enhanced haptotaxis than other cells [6]. SW620 cell had been detected tiny liver metastases in a short time, a probable explanation is that SW620 cell line has a good metastatic potential [26], which is helpful to reach and invade the liver tissue and forms metastatic nodules. The results indicated HCT116 cell and SW620 cell are suitable to develop a CRC hepatic metastases model by intra-splenic injections. As for other four CRC cell lines, compared to 0-22.2% liver metastatic rate in orthotopic transplantation group, a third to a half of tumors produced liver metastases via intra-splenic injection of cells. In addition to the advantages of the intra-splenic injections technology, another probable explanation is that the tumor cells resulted in higher death rate of mice at the beginning stage of the experiment, which were excluded from the results of statistics.

Except for observing liver metastases, we also monitored lymph node metastases, peritoneal seeding and lung metastases. HT29 cell showed 50% lymph node metastases, although it produced no liver metastases. This characteristic of the cell has been confirmed by previous work by K. Flatmark et al. [26]. We also found that HCT116 cell and LOVO cell were also with higher lymph node metastases than the corresponding ectopic transplantation group. This phenomenon suggests that modeling method of orthotopic transplantation is more likely to lead to CRC lymph node metastases. On the contrary, for intra-splenic injection group, six CRC cell lines, all of which produced widespread carcinomatosis for peritoneum, especially for HT29 cell and HCT116 cell. It cannot be ruled out contamination during the implantation procedure. For all subjects, only one case from SW620 cell gave rise to lung metastases in intra-splenic injection group. It may indicate that our modeling methods are not appropriate to form lung metastases [31].

Our study is the first time to compare the discrepancies between the two different xenograft mouse models from six CRC cell lines. It should be noticed that both the techniques and cancer cell lines have their strengths, weaknesses and significance for experimental application. Therefore, the final decision depends on the purpose of the study. Our results may be of help for other researchers to choose suitable cell lines and modeling methods for their studies in CRC tumor growth and spread.

Compliance with Ethical Standards

Conflict of Interest The authors declare that they have no conflict of interest.

Ethical Approval Animals used in research were treated humanely, and all procedures were in accordance with national and international guidelines and were approved and supervised by the Animal Care and Use Committee of Xuzhou Medical University (Jiangsu, China, permit number:2018010502).

Informed Consent Informed consent was obtained from all individual participants included in the study.

References

1. Torre LA, Bray F, Siegel RL, Ferlay J, Lortet-Tieulent J, Jemal A (2015) Global cancer statistics, 2012. CA Cancer J Clin 65(2):87–108. https://doi.org/10.3322/caac.21262
2. Arnold M, Sierra MS, Laversanne M, Soerjomataram I, Jemal A, Bray F (2017) Global patterns and trends in colorectal cancer incidence and mortality. Gut 66(4):683–691. https://doi.org/10.1136/gutjnl-2015-310912
3. Siegel R, Desantis C, Jemal A (2014) Colorectal cancer statistics, 2014. CA Cancer J Clin 64(2):104–117. https://doi.org/10.3322/caac.21220
4. O'Connell JB, Maggard MA, Ko CY (2004) Colon cancer survival rates with the new American Joint Committee on Cancer sixth edition staging. J Natl Cancer Inst 96(19):1420–1425. https://doi.org/10.1093/jnci/djh275
5. Cespedes MV, Espina C, Garcia-Cabezas MA, Trias M, Boluda A, Gomez del Pulgar MT, Sancho FJ, Nistal M, Lacal JC, Mangues R (2007) Orthotopic microinjection of human colon cancer cells in nude mice induces tumor foci in all clinically relevant metastatic sites. Am J Pathol 170(3):1077–1085. https://doi.org/10.2353/ajpath.2007.060773
6. Kazuhiro ISHIZU, Naohide SUNOSE, Kanami YAMAZAKI, Takashi TSURUO, Sotaro SADAHIRO, Hiroyasu MAKUUCHI, Takao YAMORI (2007) Development and Characterization of a Model of Liver Metastasis Using Human Colon Cancer HCT-116 Cells. Biol Pharm Bull 30:1779–1783. https://doi.org/10.1248/bpb.30.1779

7. Cho YB, Hong HK, Choi YL, Oh E, Joo KM, Jin J, Nam DH, Ko YH, Lee WY (2014) Colorectal cancer patient-derived xenografted tumors maintain characteristic features of the original tumors. J Surg Res 187(2):502–509. https://doi.org/10.1016/j.jss.2013.11.010
8. Sasaki H, Miura K, Horii A, Kaneko N, Fujibuchi W, Kiseleva L, Gu Z, Murata Y, Karasawa H, Mizoi T, Kobayashi T, Kinouchi M, Ohnuma S, Yazaki N, Unno M, Sasaki I (2008) Orthotopic implantation mouse model and cDNA microarray analysis indicates several genes potentially involved in lymph node metastasis of colorectal cancer. Cancer Sci 99(4):711–719. https://doi.org/10.1111/j.1349-7006.2008.00725.x
9. Bedard PL, Hansen AR, Ratain MJ, Siu LL (2013) Tumour heterogeneity in the clinic. Nature 501(7467):355–364. https://doi.org/10.1038/nature12627
10. Lee WY, Hong HK, Ham SK, Kim CI, CHO YB (2014) Comparison of Colorectal Cancer in differentially established liver metastasis models. Anticancer research 34(7):3321–3328
11. Roque-Lima B, Roque C, Begnami MD, Peresi P, Lima ENP, Mello CAL, Coimbra FJ, Chojniak R, Goss Santos T (2018) Development of patient-derived orthotopic xenografts from metastatic colorectal cancer in nude mice. J Drug Target:1–7. https://doi.org/10.1080/1061186X.2018.1509983
12. Nie S, Zhou J, Bai F, Jiang B, Chen J, Zhou J (2014) Role of endothelin A receptor in colon cancer metastasis: in vitro and in vivo evidence. Mol Carcinog 53 Suppl 1:E85–E91. https://doi.org/10.1002/mc.22036
13. Yang J, Shikata N, Mizuoka H, Tsuburaa A (1996) Colon carcinogenesis in shrews by intrarectal infusion of N-methyl-N-nitrosourea. Cancer letters 110:105–112. https://doi.org/10.1016/s0304-3835(96)04468-0
14. O'Rourke KP, Loizou E, Livshits G, Schatoff EM, Baslan T, Manchado E, Simon J, Romesser PB, Leach B, Han T, Pauli C, Beltran H, Rubin MA, Dow LE, Lowe SW (2017) Transplantation of engineered organoids enables rapid generation of metastatic mouse models of colorectal cancer. Nat Biotechnol 35(6):577–582. https://doi.org/10.1038/nbt.3837
15. Sloan EK, Priceman SJ, Cox BF, Yu S, Pimentel MA, Tangkanangnukul V, Arevalo JM, Morizono K, Karanikolas BD, Wu L, Sood AK, Cole SW (2010) The sympathetic nervous system induces a metastatic switch in primary breast cancer. Cancer Res 70(18):7042–7052. https://doi.org/10.1158/0008-5472.CAN-10-0522
16. Thalheimer A, Korb D, Bonicke L, Wiegering A, Muhling B, Schneider M, Koch S, Riedel SS, Germer CT, Beilhack A, Brandlein S, Otto C (2013) Noninvasive visualization of tumor growth in a human colorectal liver metastases xenograft model using bioluminescence in vivo imaging. J Surg Res 185(1):143–151. https://doi.org/10.1016/j.jss.2013.03.024
17. Terracina KP, Aoyagi T, Huang WC, Nagahashi M, Yamada A, Aoki K, Takabe K (2015) Development of a metastatic murine colon cancer model. J Surg Res 199(1):106–114. https://doi.org/10.1016/j.jss.2015.04.030
18. Trainer DL, Kline T, McCabe FL, Faucette LF, Feild J, Chaikin M, Anzano M, Rieman D, Hoffstein S, Li DJ (1988) Biological characterization and oncogene expression in human colorectal carcinoma cell lines. Int J Cancer 41:287–296. https://doi.org/10.1002/ijc.2910410221
19. Zeng Q, Lei F, Chang Y, Gao Z, Wang Y, Gao Q, Niu P, Li Q (2019) An oncogenic gene, *SNRPA1*, regulates *PIK3R1*, *VEGFC*, MKI67, CDK1 and other genes in colorectal cancer. Biomed Pharmacother. 117: https://doi.org/10.1016/j.biopha.2019.109076
20. Mittal VK, Bhullar JS, Jayant K (2015) Animal models of human colorectal cancer: Current status, uses and limitations. World J Gastroenterol 21(41):11854–11861. https://doi.org/10.3748/wjg.v21.i41.11854
21. Zigmond E, Halpern Z, Elinav E, Brazowski E, Jung S, Varol C (2011) Utilization of murine colonoscopy for orthotopic implantation of colorectal cancer. PLoS One 6(12):e28858. https://doi.org/10.1371/journal.pone.0028858
22. Golovko D, Kedrin D, Yilmaz OH, Roper J (2015) Colorectal cancer models for novel drug discovery. Expert Opin Drug Discov 10(11):1217–1229. https://doi.org/10.1517/17460441.2015.1079618
23. Hackl C, Man S, Francia G, Milsom C, Xu P, Kerbel RS (2013) Metronomic oral topotecan prolongs survival and reduces liver metastasis in improved preclinical orthotopic and adjuvant therapy colon cancer models. Gut 62(2):259–271. https://doi.org/10.1136/gutjnl-2011-301585
24. Hite N, Klinger A, Hellmers L, Maresh GA, Miller PE, Zhang X, Li L, Margolin DA (2018) An Optimal Orthotopic Mouse Model for Human Colorectal Cancer Primary Tumor Growth and Spontaneous Metastasis. Dis Colon Rectum 61(6):698–705. https://doi.org/10.1097/DCR.0000000000001096
25. Valastyan S, Weinberg RA (2011) Tumor metastasis: Molecular insights and evolving paradigms. Cell 147:275–292. https://doi.org/10.1016/j.cell.2011.09.024
26. Flatmark K, Maelandsmo GM, Martinsen M, Rasmussen H, Fodstad O (2004) Twelve colorectal cancer cell lines exhibit highly variable growth and metastatic capacities in an orthotopic model in nude mice. Eur J Cancer 40(10):1593–1598. https://doi.org/10.1016/j.ejca.2004.02.023
27. Rajput A, Dominguez San Martin I, Rose R, Beko A, Levea C, Sharratt E, Mazurchuk R, Hoffman RM, Brattain MG, Wang J (2008) Characterization of HCT116 human colon cancer cells in an orthotopic model. J Surg Res 147(2):276–281. https://doi.org/10.1016/j.jss.2007.04.021
28. Beauchemin N (2011) The colorectal tumor microenvironment: the next decade. Cancer Microenviron 4(2):181–185. https://doi.org/10.1007/s12307-011-0074-7
29. Qin JZ, Upadhyay V, Prabhakar B, Maker AV (2013) Shedding LIGHT TNFSF14 on the tumor microenvironment of colorectal cancer liver metastases. Journal of translational medicine 11:1–10. https://doi.org/10.1186/1479-5876-11-70
30. Bocuk D, Wolff A, Krause P, Salinas G, Bleckmann A, Hackl C, Beissbarth T, Koenig S (2017) The adaptation of colorectal cancer cells when forming metastases in the liver: expression of associated genes and pathways in a mouse model. BMC Cancer 17:1–15
31. Lu Y, Zhao X, Li K, Luo G, Nie Y, Shi Y, Zhou Y, Ren G, Feng B, Liu Z, Pan Y, Li T, Guo X, Wu K, Miranda-Vizuete A, Wang X, Fan D (2013) Thioredoxin-like protein 2 is overexpressed in colon cancer and promotes cancer cell metastasis by interaction with ran. Antioxid Redox Signal 19(9):899–911. https://doi.org/10.1089/ars.2012.4736

Publisher's Note Springer Nature remains neutral with regard to jurisdictional claims in published maps and institutional affiliations.